BIOCHEMISTRY
including biophysical chemistry & molecular biology

Article

pubs.acs.org/biochemistry

Location of the Synaptosome-Binding Regions on Botulinum Neurotoxin B

Behzod Z. Dolimbek,[†] Lance E. Steward,[‡] K. Roger Aoki,[‡] and M. Zouhair Atassi*[,†,§]

[†]Department of Biochemistry and Molecular Biology, Baylor College of Medicine, Houston, Texas 77030, United States
[‡]The Neurotoxin Research Program, Department of Biological Sciences, Allergan, Inc., Irvine, California 92612, United States
[§]Department of Pathology and Immunology, Baylor College of Medicine, Houston, Texas 77030, United States

Supporting Information

ABSTRACT: The regions of botulinum neurotoxin B (BoNT/B) involved in binding to mouse brain synaptosomes (snps) were localized. Sixty 19-residue overlapping peptides (peptide C31 consisted of 24 residues) encompassing BoNT/B H chain (residues 442−1291) were synthesized and used to inhibit binding of ^{125}I-labeled BoNT/B to snps. Synaptosome-binding regions were noncompeting and existed on both H_N and H_C domains of neurotoxin. At 37 °C, inhibitory activities on H_N resided, in decreasing order, in peptides 638−656 (26.7%), 596−614 (18.2%), 512−530 (13.9%), 778−796 (13.8%), and 526−544 (11.6%). On H_C, activity resided in decreasing order in peptides 1170−1188 (44.6%), 1128−1146 (21.6%), 1184−1202 (18.6%), 1156−1174 (13.0%), 946−964 (11.8%), 1114−1132 (11.2%), 1100−1118 (6.2%), 876−894 (6.1%), 1268−1291 (4.6%), and 1226−1244 (4.3%). The 45 remaining H_N and H_C peptides had no activity. At 4 °C, peptide C24 (1170−1188) remained quite active (inhibiting, 31.2%), while activities of peptides N15, C21, and C25 were little under 10%. The snp-binding regions contained sites that bind synaptotagmin II and gangliosides. Despite the low degree of sequence homology, BoNT/B and BoNT/A display significant structural homology and appeared to bind in part to the same snp-binding regions. Binding of each labeled toxin to snps was inhibited ∼50% by the other toxin, 70−72% by its correlate H_C, and by the H_C of the other toxin [29% (BoNT/A by H_C of B) or 32% (BoNT/B by H_C of A)]. In the three-dimensional structure of BoNT/B, the greater part of H_C, one H_N face, and part of the belt on the same side interact with snps. Thus, BoNT/B binds to snps through the H_C head and employs regions on one H_N face and the belt, reserving flexibility for the belt's unbound part to release the light chain. Most snp-binding regions coincide or overlap with blocking antibody (Ab)-binding regions explaining how such Abs prevent BoNT/B toxicity.

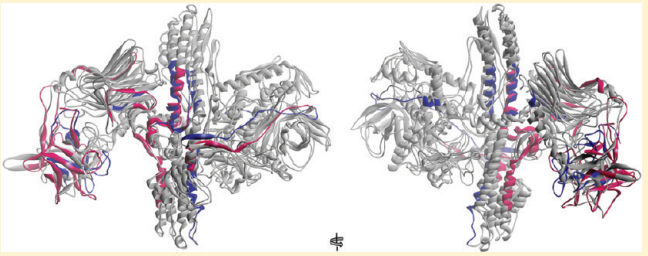

Botulinum neurotoxins (BoNTs) are 150 kDa extremely toxic proteins produced by *Clostridium botulinum* in seven immunological serotypes (A−G). They cause botulism in humans (serotypes A, B, and E) and other mammals (serotypes C, D, and F). Botulinum neurotoxin acts on the nervous system by blocking the release of acetylcholine from nerve terminals at the neuromuscular junction and thus causes paralysis. The action of BoNT is initiated by its binding to a receptor molecule on the nerve cell surface, and the toxin−receptor complex undergoes endocytosis. The L chain is a zinc endopeptidase,[1] and once inside the cell, it cleaves a SNARE protein (soluble *N*-ethylmaleimide-sensitive factor attachment protein receptor) essential for vesicle docking and fusion and as a result neurotransmitter release is reduced.[2] Each serotype cleaves a particular peptide bond on one or more of the SNARE proteins.[3]

BoNTs bind to brain synaptosomes (snps) of various species.[4−17] Internalization of BoNT is receptor-mediated, and different BoNTs use distinct receptors on motor nerves.[13,18,19] It has been shown that BoNT/B binds to synaptotagmin (a synaptic vesicle membrane protein) in association with ganglioside GT1b or GD1a.[10] GT1b is a part of the receptor complex for both neurotoxins A and B.[20] Both synaptotagmins I and II function as receptors for BoNT/B.[11,12,20−22] The affinities of BoNT/B for synaptotagmins I and II are similar to the binding affinities for snps.[11] It has been proposed that specific gangliosides associate with the N-terminal domain of synaptotagmin II to form the binding site for BoNT/B.[11,12] Different strains of BoNT/B have been reported to bind with different affinities to synaptotagmin II in association with GT1b.[23] It has recently been demonstrated[22] that synaptotagmins I and II mediated entry of BoNT/B (but not BoNT/A or BoNT/E) into PC12 cells. Recently, the binding surfaces between BoNT/B and rat[24] or mouse[25] synaptotagmin II were determined by X-ray crystallography.

There is evidence that the binding of BoNT/A and BoNT/B to snps takes place via the H chain.[9,10,26−28] Cleavage of the H chain of BoNT/A by mild trypsin action on BoNT produced a 46 kDa C-terminal fragment (H_C) and a 49 kDa N-terminal fragment attached to the L chain by the interchain disulfide bond

Received: August 19, 2011
Revised: December 2, 2011
Published: December 6, 2011

Table 1. Synthetic Overlapping Peptides of the BoNT/B Heavy Chain[a]

Peptide	Residue Numbers	Amino acid sequence
H_N domain Peptides		
N1	442-460	APGICIDVDNEDLF**FIADK**
N2	456-474	**FIADK**NSFSDDLSK**NERIE**
N3	470-488	**NERIE**YNTQSNYIE**NDFPI**
N4	484-502	**NDFPI**NELILDTDL**ISKIE**
N5	498-516	**ISKIE**LPSENTESL**TDFNV**
N6	512-530	**TDFNV**DVPVYEKQP**AIKKI**
N7	526-544	**AIKKI**FTDENTIFQ**YLYSQ**
N8	540-558	**YLYSQ**TFPLDIRDI**SLTSS**
N9	554-572	**SLTSS**FDDALLFSN**KVYSF**
N10	568-586	**KVYSF**FSMDYIKTA**NKVVE**
N11	582-600	**NKVVE**AGLFAGWVK**QIVND**
N12	596-614	**QIVND**FVIEANKSN**TMDKI**
N13	610-628	**TMDKI**ADISLIVPY**IGLAL**
N14	624-642	**IGLAL**NVGNETAKG**NFENA**
N15	638-656	**NFENA**FEIAGASIL**LEFIP**
N16	652-670	**LEFIP**ELLIPVVGA**FLLES**
N17	666-684	**FLLES**YIDNKNKII**KTIDN**
N18	680-698	**KTIDN**ALTKRNEKW**SDMYG**
N19	694-712	**SDMYG**LIVAQWLST**VNTQF**
N20	708-726	**VNTQF**YTIKEGMYK**ALNYQ**
N21	722-740	**ALNYQ**AQALEEIIK**YRYNI**
N22	736-754	**YRYNI**YSEKEKSNI**NIDFN**
N23	750-768	**NIDFN**DINSKLNEG**INQAI**
N24	764-782	**INQAI**DNINNFING**CSVSY**
N25	778-796	**CSVSY**LMKKMIPLA**VEKLL**
N26	792-810	**VEKLL**DFDNTLKKN**LLNYI**
N27	806-824	**LLNYI**DENKLYLIG**SAEYE**
N28	820-838	**SAEYE**KSKVNKYLK**TIMPF**
N29	834-852	**TIMPF**DLSIYTNDT**ILIEM**
H_C domain		
C1	848-866	**ILIEM**FNKYNSEIL**NNIIL**
C2	862-880	**NNIIL**NLRYKDNNL**IDLSG**
C3	876-894	**IDLSG**YGAKVEVYD**GVELN**
C4	890-908	**GVELN**DKNQFKLTS**SANSK**
C5	904-922	**SANSK**IRVTQNQNI**IFNSV**
C6	918-936	**IFNSV**FLDFSVSFW**IRIPK**
C7	932-950	**IRIPK**YKNDGIQNY**IHNEY**
C8	946-964	**IHNEY**TIINCMKNN**SGWKI**
C9	960-978	**SGWKI**SIRGNRIIW**TLIDI**
C10	974-992	**TLIDI**NGKTKSVFF**EYNIR**
C11	988-1006	**EYNIR**EDISEYINR**WFFVT**
C12	1002-1020	**WFFVT**ITNNLNNAK**IYING**
C13	1016-1034	**IYING**KLESNTDIK**DIREV**
C14	1030-1048	**DIREV**IANGEIIFK**LDGDI**
C15	1044-1062	**LDGDI**DRTQFIWMK**YFSIF**
C16	1058-1076	**YFSIF**NTELSQSNI**EERYK**
C17	1072-1090	**EERYK**IQSYSEYLK**DFWGN**
C18	1086-1104	**DFWGN**PLMYNKEYY**MFNAG**
C19	1100-1118	**MFNAG**NKNSYIKLK**KDSPV**
C20	1114-1132	**KDSPV**GEILTRSKY**NQNSK**
C21	1128-1146	**NQNSK**YINYRDLYI**GEKFI**
C22	1142-1160	**GEKFI**IRRKSNSQS**INDDI**
C23	1156-1174	**INDDI**VRKEDYIYL**DFFNL**
C24	1170-1188	**DFFNL**NQEWRVYTY**KYFKK**
C25	1184-1202	**KYFKK**EEEKLFLAP**ISDSD**
C26	1198-1216	**ISDSD**EFYNTIQIK**EYDEQ**
C27	1212-1230	**EYDEQ**PTYSCQLLF**KKDEE**
C28	1226-1244	**KKDEE**STDEIGLIG**IHRFY**
C29	1240-1258	**IHRFY**ESGIVFEEY**KDYFC**
C30	1254-1272	**KDYFC**ISKWYLKEV**KRKPY**
C31	1268-1291	**KRKPY**NLKLGCNWQ FIPKDEGWTE

[a]We previously reported the synthesis of 60 overlapping peptides of the BoNT/B heavy chain.[32] They encompass the entire amino acid sequence of the BoNT/B heavy chain (residues 442−1291) and were 19 residues each (except for peptide C31, which was 24 residues long) and overlapped consecutively by five residues. The overlap sequences between consecutive peptides are shown in bold and underlined.

dx.doi.org/10.1021/bi201322c | *Biochemistry* 2012, 51, 316−328

(i.e., a 101 kDa fragment).[29,30] The H_N−L fragment produced by trypsin did not bind to snps, leading to the view that the toxin-binding site resided in the C-terminal half of the H chain.[29]

Clearly, binding of BoNTs to their cell surface receptors is a requisite for toxicity. Understanding the binding events and the toxin regions involved will be essential for devising interfering molecular strategies for blocking binding and preventing toxicity. We have previously determined the locations of the snp-binding sites on BoNT/A.[31] In this work, we have determined the regions of BoNT/B that are involved in the binding of the neurotoxin to snps. To do this, we prepared and used a panel of uniformly sized synthetic overlapping peptides that encompassed the entire 850-residue subunit and determined their activities in inhibition of active BoNT/B binding to mouse brain snps.

MATERIALS AND METHODS

Botulinum Neurotoxins, Synthetic BoNT/B Peptides, Recombinant BoNT/B Domains and Animals. Active BoNT/A and BoNT/B were purchased from Metabiologics (Madison, WI) as solutions (0.25 mg/mL) in PBS containing 25% glycerol and stored at −20 °C. We used the 60 consecutive overlapping peptides (Table 1) that comprise the entire sequence of the H subunit (residues 442−1291) of BoNT/B. Synthesis, purification, and characterization of the peptides have been described previously.[32] The peptides are 19 residues long (except for peptide C31, which is 24 residues long) and overlap consecutively by five residues. Recombinant H_C of BoNT/B and the L chain were gifts from L. A. Smith (U.S. Army Medical Research and Materiel Command, Fort Detrick, MD). Outbred mice (ICR), 4−6 weeks old, were purchased from the Center for Comparative Medicine of the Baylor College of Medicine (Houston, TX) and were kept before use in our in-house animal facility until they were 7−9 weeks old.

Preparation of Synaptosomes. This work has been conducted in strict accordance with the guidelines in the Guide for the Care and Use of Laboratory Animals. The animal protocol was approved by the Institutional Animal Care and Use Committee of the Baylor College of Medicine (protocol AN-3018). Synaptosomes were isolated from mouse brain as described by Whittaker,[33] with minor changes. Nine ICR mice (24−26 g) were sacrificed by cervical dislocation; their brains were extracted (yield of 3.7 g, i.e., 0.41 g/mouse) and transferred to a sterile Petri dish at 0 °C with 8 mL of 0.32 M sucrose buffer containing 10 mM Tris (pH 7.0). All other steps were conducted at 4 °C. The brains [in 35 mL of 0.32 M sucrose buffer containing 10 mM Tris (pH 7.0)] were homogenized using a Glenco glass/Teflon homogenizer (280 mL) and a Con-Torque Electric Power Unit (Eberbach Corp., Ann Arbor, MI) at 800 rpm of pestle with 10 strokes in and out. The pinkish suspension was transferred equally into two 30 mL plastic Beckman screw-cup tubes and centrifuged (1000*g* for 10 min) in a Beckman J2-21M/E centrifuge using a JA-17 rotor to remove the precipitate that mostly consisted of cellular debris and nuclear fraction. The supernatant (~35 mL) was divided into four plastic 10 mL Beckman screw-cup tubes (~8.75 mL/tube) and centrifuged (26000*g* for 17 min) on a JA-21 rotor to yield the crude pellet of snps. The pellet was washed with 9 mL of 0.32 M sucrose buffer containing 10 mM Tris (pH 7.0). An aliquot (3.5 mL) of 0.32 M sucrose buffer containing 10 mM Tris (pH 7.0) was added to each tube and gently mixed with pipetting in and out, and the suspensions in the four tubes were combined. An aliquot (2.33 mL, one-sixth) of this suspension was carefully layered onto a gradient from 3 mL of 0.8 M sucrose [containing 10 mM Tris (pH 7.0)] to 3 mL of 1.2 M sucrose [containing 10 mM Tris (pH 7.0)], prepared immediately before use in a plastic 10 mL Beckman tube. The layers were centrifuged (26000*g* for 210 min) at 4 °C using the JA-21 rotor. The grayish-tan material between 0.8 and 1.2 M buffers was collected (6 mL), resuspended with 8 mL of 0.14 M NaCl containing 10 mM Tris buffer (pH 7.0) (saline/Tris), and centrifuged for 17 min at 26000*g* at 4 °C using the JA-21 rotor. The pellet was washed twice with the same buffer to remove traces of sucrose, and the synaptosomes (wet packed volume of 1.4 mL) were resuspended in 87.5 mL of saline/Tris (stock suspension of snps). The snp protein concentration was determined by binding to Coomassie Brilliant Blue G-250 as described previously[34] and stored frozen at −80 °C until it was used in a binding or inhibition assay.

Preparation of ^{125}I-Labeled BoNT/B and the Synaptosome Binding Assay. Active BoNT/B (20 μg) was labeled with ^{125}I using the chloramine T method[35] in a safe laboratory setting and procedures that protect from direct radioactivity and exposure to active BoNT. The labeled product was passed through a Sephadex G-25 M column [in Ringer's buffer containing 120 mM NaCl, 2.5 mM KCl, 2 mM $CaCl_2$, 4 mM $MgCl_2$, 5 mM Tris, and 0.5% BSA (pH 7.0)] to remove excess unbound radioactive iodine from ^{125}I-labeled BoNT/B. The labeled toxin was stored at 0 °C and used within 5−7 days. Increasing amounts of snps (1−900 μg/mL of snp protein) in triplicate were incubated with ^{125}I-labeled active BoNT/B (50000 cpm, ~2 ng) at 37 °C for different periods of time under isotonic conditions in 0.1 mL of Ringer's buffer. The time course (from 5 to 240 min) of interaction of a fixed amount of snps (105.0 μg/mL of snp protein) with [^{125}I]BoNT/B (50000 cpm) was also studied. The reaction mixture was centrifuged (20000*g* and 20 °C) for 3 min followed by aspiration of the supernatant and washing twice by centrifugation with 1.0 mL of Ringer's isotonic buffer. The supernatant was removed to leave the snp pellet dotted on the bottom of a 1.5 mL plastic tube. The bottoms of the tubes with snps were cut out and the samples transferred to clean glass tubes. The incorporated radioactivity was measured in an Automatic Gamma Counter (1277 Gammamaster, LKB-Wallac, Turku, Finland).

Inhibition of the Binding of ^{125}I-Labeled BoNT/A or ^{125}I-Labeled BoNT/B to Synaptosomes with Correlated Unlabeled Toxin or Domains. Triplicate samples of a fixed amount of snps (105.0 μg/mL of snp protein) were incubated (60 min at 37 °C) in Ringer's solution with increasing amounts (6.67×10^{-4} to 53.33×10^{-4} nmol) of unlabeled inhibitors. The inhibitors were active BoNT/B, active BoNT/A, recombinant H_C (rH_C) of BoNT/B, recombinant H_C (rH_C) of BoNT/A, and recombinant L chain (rLC) of BoNT/B. [^{125}I]BoNT/B or [^{125}I]BoNT/A (50000) was then added, and after the reaction had proceeded for 10 min at 37 °C, inhibited snps and uninhibited controls were centrifuged (20000*g* for 3 min). The supernatant was removed, and the pellets were washed twice on the centrifuge with 1.0 mL of Ringer's solution. After aspiration of the supernatants, the plastic tube bottoms were cut out into clean glass tubes and the samples counted on a gamma counter. The amounts of bound [^{125}I]BoNT/B or [^{125}I]BoNT/A from inhibited samples relative to uninhibited controls were expressed as the percent inhibition.

Inhibition Assay with Individual Synthetic Toxin Peptides. Inhibition with the individual peptides was conducted at two temperatures, 37 and 4 °C. We determined at

these two temperatures the ability of each synthetic BoNT/B H chain peptide to inhibit the binding of ^{125}I-labeled BoNT/B to snps. Increasing amounts of peptide (0.045−0.136 nmol, in Ringer's solution) were incubated (20 min at 37 or 4 °C) with snps (105.0 μg/mL of snp protein). ^{125}I-labeled toxin (50000 cpm) was added to the mixture and allowed to react at 37 °C for 10 min. The samples were centrifuged (20000*g* for 3 min) and supernatants discarded. The pellets were washed on the centrifuge twice with 1.0 mL of Ringer's solution. The washed snps with bound ^{125}I-labeled BoNT/B in inhibited samples and uninhibited controls were transferred to glass tubes by cutting out the tube bottoms and counted on a gamma counter. We also performed a time course inhibition with a fixed amount of the H chain peptides (0.136 nmol) of the binding of ^{125}I-labeled BoNT/B to snps under the conditions described above. Inhibition at 4 °C with the active H chain peptides (0.136 nmol) of the binding of ^{125}I-labeled BoNT/B to snps was also conducted as a time course study. The values obtained at 60 min in both time course studies were plotted after subtraction by the respective average of internal negative peptide controls. All experiments were conducted in triplicate.

Inhibition with Equimolar Mixtures of the Active Peptides. Mixtures of equimolar amounts of active inhibitory peptides were tested in a time course assay for their inhibition of BoNT/B−snp binding. Three mixtures contained the following H_N, H_C, or H chain peptides: (1) a mixture of active H_N peptides N6, N12, N15, and N25 (0.034 nmol each), (2) a mixture of active H_C peptides C3, C8, C21, C24, C28, and C31 (0.0227 nmol each), and (3) a mixture of all 10 peptides, N6, N12, N15, N25, C3, C8, C21, C24, C28, and C31 (0.0136 nmole each). A peptide mixture (0.136 nmol of total peptide in Ringer's buffer) was incubated with snps (105.0 μg/mL protein, 37 °C) for 20, 40, 60, 120, or 240 min. ^{125}I-labeled BoNT/B (50000 cpm) was then added. The reaction was allowed to continue for 10 min at 37 °C, after which the mixture was centrifuged (20000*g* for 3 min at 20 °C). The supernatants were aspirated, and the snp pellets were washed on the centrifuge twice with 1.0 mL of Ringer's solution. The snp pellets were transferred to glass tubes by cutting out the tube bottoms, and their radioactivity was counted in a gamma counter. All experiments were conducted in triplicate.

RESULTS

Stability of Synaptosome Binding. A time course study was performed of the binding of labeled BoNT/B (50000 cpm) with a fixed amount of snps (105 μg/mL). The stability of the snp preparation was determined by binding of [^{125}I]BoNT/B (50000 cpm/0.1 mL, 10 min). After a period of 80 h, the binding activity decreased to 86.3% (Figure 1). However, within the time frame of the experiments in these studies (i.e., 1−2 h), the binding activity decreased only very slightly (1 h, 98.9%; 2 h, 98.3%).

Binding of ^{125}I-Labeled BoNT/B or BoNT/A to Synaptosomes and Inhibition by Toxins and Domains. A fixed amount of ^{125}I-labeled BoNT/B (50000 cpm) was allowed to react with increasing amounts of snps (in the range of 1−900 μg/mL of snp protein). The results are shown in Figure 2. The amount of [^{125}I]BoNT/B bound to snps increased with time to around 18% of the added toxin at ∼225 μg/mL snp protein (Figure 2a). When fixed amounts of [^{125}I]BoNT/B (50000 cpm) and snps (105 μg/mL) were allowed to interact in a time course study, binding reached a plateau at ∼60 min (Figure 2b). Figure 3 shows the inhibitions of the binding of labeled BoNT/B to snps by unlabeled BoNT/B, unlabeled BoNT/A, and the BoNT/B domains. As expected, BoNT/B completely inhibited the binding

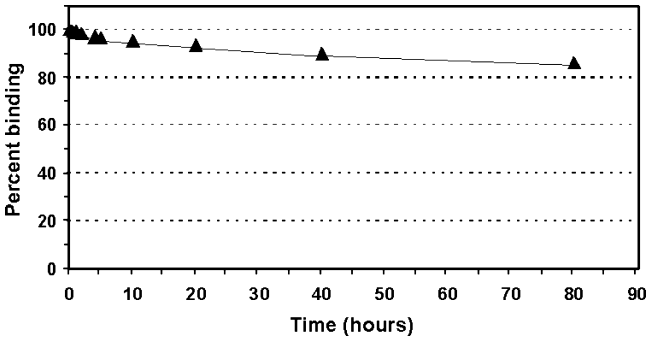

Figure 1. Stability of snps in Ringer's buffer at 37 °C tested by storage of snps at 37 °C for up to 80 h. Aliquots (105.00 μg/mL protein) were taken at the indicated time intervals and reacted with [^{125}I]BoNT/B (50000 cpm/0.1 mL, 10 min). The decrease in the percent binding with [^{125}I]BoNT/B was calculated relative to a freshly thawed control snp sample (105.00 μg/mL).

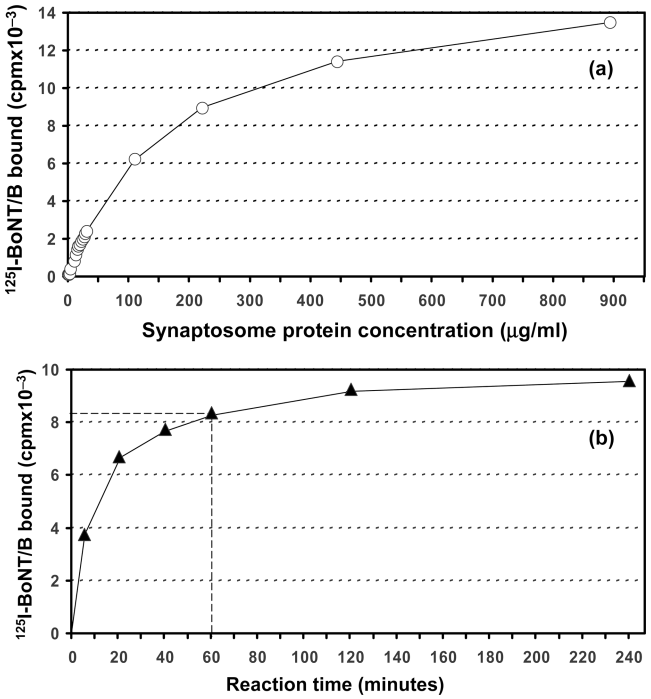

Figure 2. (a) Binding of ^{125}I-labeled active BoNT/B to increasing amounts of snps. A fixed amount of ^{125}I-labeled BoNT/B (50000 cpm, ∼2 ng) was reacted (20 min, 37 °C, triplicate reactions) with increasing amounts (1−900 μg/mL protein) of synaptosomes in 0.1 mL of Ringer's solution. The mixture was centrifuged for 3 min (20000*g* at 20 °C), and the supernatant was aspirated before the pellets were washed twice by centrifugation with 1.0 mL of Ringer's solution. The bottoms of tubes with snp pellets were cut into clean glass tubes, and the incorporated radioactivity was measured. (b) Time course of binding of ^{125}I-labeled active BoNT/B (50000 cpm) with snps at a fixed snp protein concentration (105.00 μg/mL).

of labeled BoNT/B. Unlabeled BoNT/A inhibited the binding of BoNT/B by ∼50% (Figure 3a,b), and conversely, unlabeled BoNT/B inhibited the binding of BoNT/A by 48% (Figure 3c,d). The binding of ^{125}I-labeled BoNT/B was inhibited by a maximum of ∼32% by rH_C of BoNT/A. Conversely, ^{125}I-labeled BoNT/A binding was also inhibited 29% by rH_C of BoNT/B. The binding of labeled BoNT/B was inhibited 71% by its correlated unlabeled rH_C of BoNT/B (Figure 3a,b). Similarly, the binding of BoNT/A was inhibited by 70% by rH_C of BoNT/A (Figure 3c,d).

dx.doi.org/10.1021/bi201322c | *Biochemistry* 2012, 51, 316−328

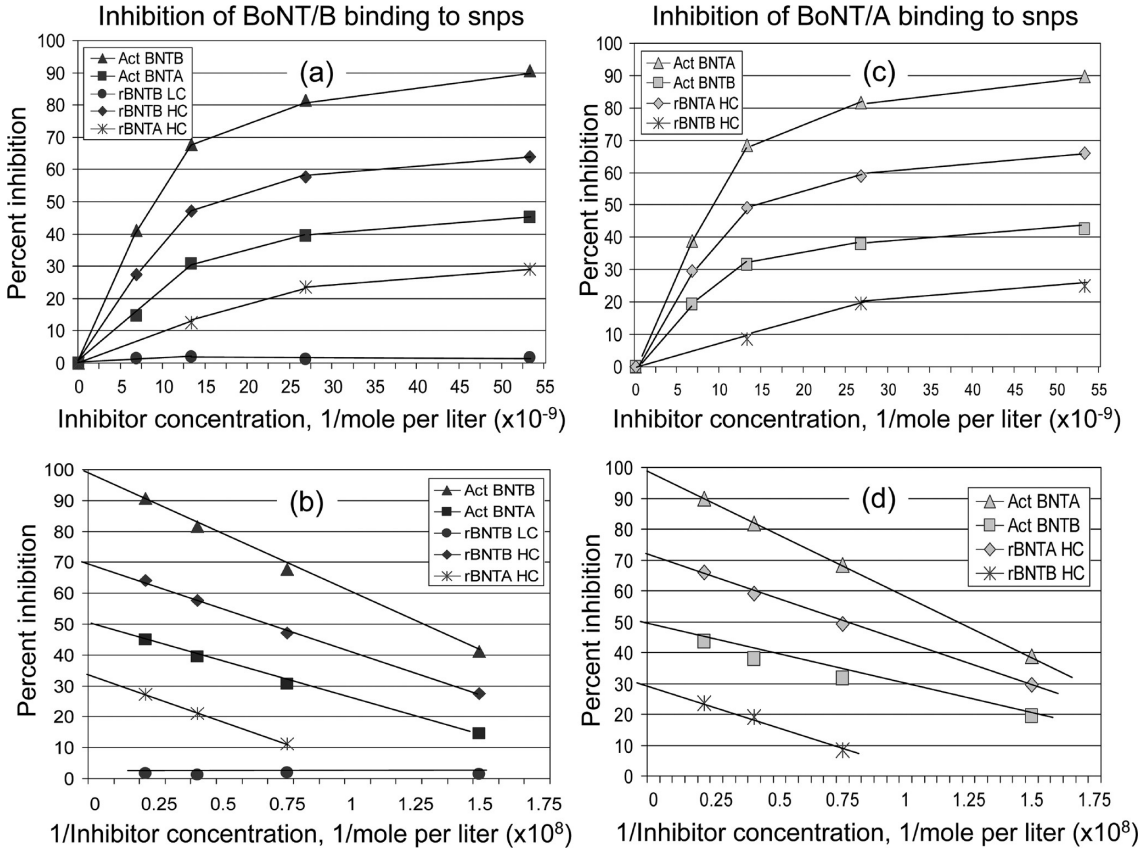

Figure 3. (a and b) Inhibition of the binding of ^{125}I-labeled active BoNT/B to snps by active BoNT/B, active BoNT/A, rH_C of BoNT/B, rH_C of BoNT/A, or recombinant BoNT/B L chain. (c and d) Inhibition of the binding of ^{125}I-labeled active BoNT/A to snps by active BoNT/A, active BoNT/B, rH_C of BoNT/A, or rH_C of BoNT/B. Snps (10.5 μg of snp protein) were incubated with increasing amounts of unlabeled inhibitors (60 min at 37 °C), in at least triplicate per inhibitor concentration, followed by reaction with ^{125}I-labeled BoNT/B or ^{125}I-labeled BoNT/A (50000 cpm for 10 min at 37 °C) in 0.1 mL of Ringer's solution. The percent inhibition was calculated from the binding results of ^{125}I-labeled BoNT/B or ^{125}I-labeled BoNT/A in the presence of inhibitors relative to uninhibited controls. (a and c) Percent inhibition with increasing amounts of inhibitors. (b and d) Percent inhibition values plotted as a function of the reciprocal of the inhibitor concentration.

In contrast, unlabeled rLC of BoNT/B had no activity upon binding of [^{125}I]BoNT/B to snps (Figure 3a,b).

Inhibition by the Individual Peptides of the Binding of ^{125}I-Labeled BoNT/B to Synaptosomes. We determined the abilities of the individual BoNT/B peptides (0.1 μg/100 μL and higher concentrations) to inhibit the binding of ^{125}I-labeled BoNT/B to snps. At 37 °C, optimal inhibitory activities were obtained at a peptide concentration of 0.3 μg/100 μL (1.4×10^{-6} M). The time course inhibition curves of active peptides are shown in Figure 4. The inhibition was essentially at, or near, a plateau at 60 min. The other 44 peptides (not shown in Figure 4) displayed inhibition values that were similar to values of nonspecific binding (<10%) and were used as internal negative controls. At 4 °C, time course inhibition of the active peptides also was at a plateau within 60 min. Figure 5 compares the inhibition results at 37 and 4 °C. The net inhibition values of the active peptides (inhibition above 10%) were obtained by subtraction of an average of the internal negative peptid controls. Several inhibitory regions are located on both the H_C and H_N domains (Figure 5). At 37 °C, the inhibitory activities are exhibited, in decreasing order, by peptides N15 (26.7%), N12 (18.2%), N6 (13.9%), N25 (13.8%), and N7 (11.6%). The other 24 H_N peptides had no inhibitory activity. The H_C domain contains clusters of snp-binding regions that are in decreasing order of activity C24 (44.6%), C21 (21.6%), and C25 (18.6%), followed in activity by peptides C8, C20, and C23 (between 11.2 and 13.0%). The other five peptides, C3, C19, C26, C28, and C31, had inhibitory activities between 3.7 and 6.2%. The remaining 20 H_C peptides showed no inhibitory activity. In the inhibition at 4 °C (Figure 5), only peptide C24 retained considerable inhibitory activity (31.2%), and levels of inhibition by peptides N15 (9.5%), C21 (9.13%), or C25 (9.87%) fell slightly below 10%. The activity at 4 °C of the remaining peptides that were active at 37 °C fell to ≤5% (Figure 5).

Inhibition of the Binding of ^{125}I-Labeled BoNT/B to Synaptosomes by Mixtures of Peptides. We also determined the inhibitory activities of [^{125}I]BoNT/B binding to snps by equimolar mixtures of active H_N or H_C peptides: (1) H_N peptides N6, N12, N15, and N25, (2) H_C peptides C3, C8, C21, C24, C28, and C31, and (3) all 10 peptides, N6, N12, N15, N25, C3, C8, C21, C24, C28, and C31. The total amount of inhibiting peptides used per assay was kept at 0.3 μg/100 μL of reaction mixture. Figure 6 shows a time course assay of the inhibitory activities of the three mixtures. Inhibitions by the peptide mixtures reached a plateau at 60 min. The level of inhibition of the binding of the toxin to snps by the H_N peptide mixture was 32.0%. The level of inhibition by the H_C peptides was, as expected, stronger (52.2%). The mixture of the 10 peptide regions exhibited an inhibitory activity of 58.5% (Figure 6).

DISCUSSION

The inability of BoNT to bind to the presynaptic cell surface prevents the toxin from exerting its potent toxicity. The aim of

dx.doi.org/10.1021/bi201322c | *Biochemistry* 2012, 51, 316−328

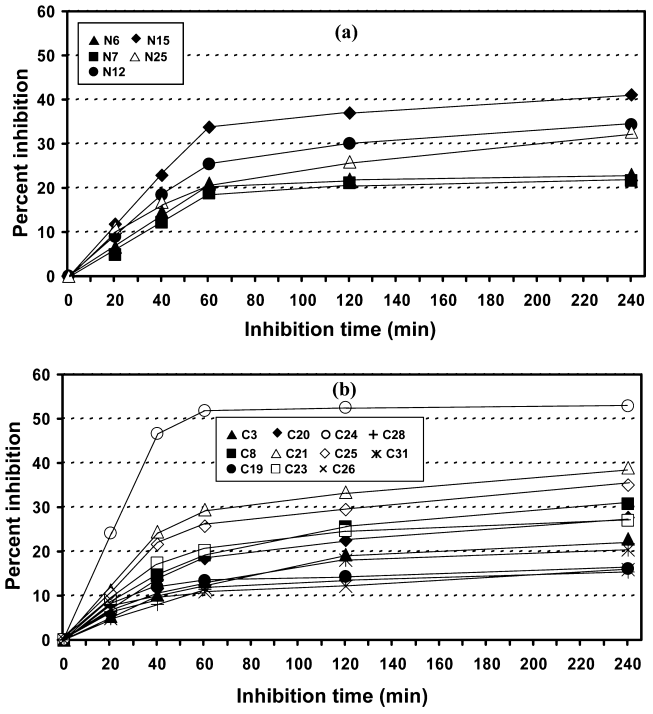

Figure 4. Inhibition of the binding of ^{125}I-labeled active BoNT/B to snps by (a) individual H_N domain peptides or (b) individual H_C domain peptides of BoNT/B. Snps (10.5 μg of snp protein) and a fixed amount of inhibitor peptides (13.75×10^{-7} mol/L) were reacted at 37 °C followed by reaction with ^{125}I-labeled toxin (50000 cpm for 10 min at 37 °C) in 0.1 mL of Ringer's solution. The percent inhibition was calculated from the values in inhibited reactions relative to uninhibited controls.

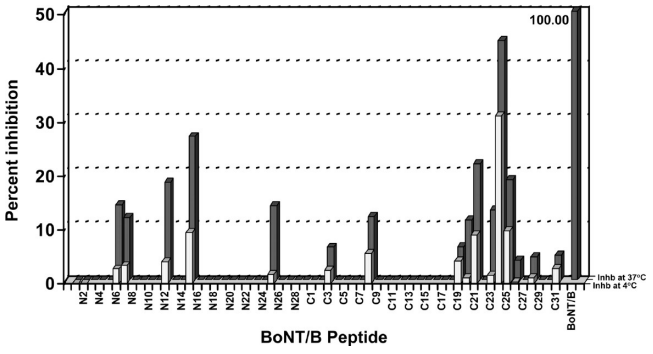

Figure 5. Regions on the heavy chain of BoNT/B that bind to mouse brain synaptosomes. The maximal values in a time course inhibition at 37 °C (dark gray bars) of the binding of [^{125}I]BoNT/B to snps (60 min inhibition values in Figure 4) by the 60 individual H chain peptides subtracted by an average value of internal control peptides are plotted as a bar diagram. The inhibition results at 4 °C subtracted by an average value from internal controls are shown as white bars.

this work was to identify the snp-binding regions on BoNT/B, which should provide information about the mechanism of action of this neurotoxin and assist in the design of synthetic peptide vaccines that incorporate snp-binding regions in the constructs. Antibodies against correctly designed peptides should block binding and disable the toxin.

Injection of BoNTs into a muscle causes a reversible partial neuromuscular junction paralysis. This ability is exploited successfully for treating a variety of clinical conditions associated with involuntary muscle spasm and contractions as

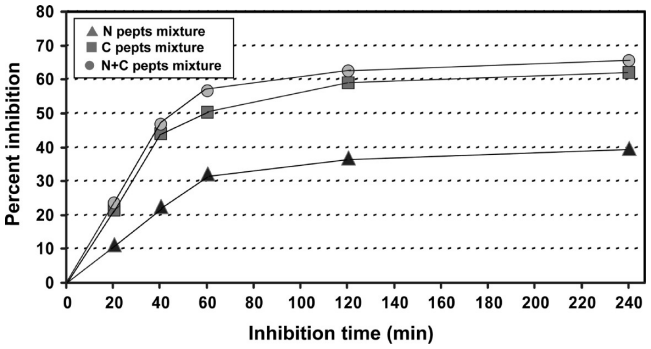

Figure 6. Inhibition of the binding of [^{125}I]BoNT/B to snps by mixtures of equimolar quantities (total peptide concentration of 13.75×10^{-7} mol/L) of the BoNT/B peptides: four H_N peptides (N6, N12, N15, and N25), six H_C peptides (C3, C8, C21, C24, C28, and C31), and 10 H chain peptides (N6, N12, N15, N25, C3, C8, C21, C24, C28, and C31). Other experimental conditions were as described in the legend of Figure 4.

well as in cosmetic and other therapeutic applications.[36−45] Because the blockade is reversible, the therapeutic benefits are transient and repeat BoNT injections are required. As a result, the treatment may elicit, in some patients, blocking antitoxin Abs that weaken or completely prevent the patient's responsiveness to further treatment.[46−48] Information about the positions of the snp-binding regions and the regions recognized by the blocking Abs of the patients presents peptide candidates that may be exploited in epitope specific containment of the Abs against these regions,[49,50] thereby allowing extension of the beneficial treatment.

Our recent localization of the Ab recognition regions on BoNT/B demonstrated[32,51] that blocking Abs bound to regions in the H_C and H_N domains. Furthermore, previous mapping of the snp-binding regions on BoNT/A[31] established that the toxin employs regions on the H_C and H_N domains for binding to and translocation into the cell. Therefore, we decided in this work to examine the entire BoNT/B molecule.

Initial experiments were conducted to determine the optimal experimental conditions, using a fixed amount of ^{125}I-labeled BoNT/B (50000 cpm) and increasing amounts of snps (1−900 μg/mL protein). It was found that the level of binding of BoNT/B increased as the amount of snps increased and approached a plateau at >500 μg of snp protein/mL (Figure 2a). In the time course study, the amount of snps corresponding to 105 μg of protein/mL was used and resulted (at 60 min) in values between 8000 and 9000 bound counts per minute.

It showed that binding approached a plateau at ∼120 min and was ∼90% complete at 60 min. In all subsequent studies, binding was conducted for 60 min. As expected, unlabeled BoNT/B inhibited completely (100%) labeled BoNT/B binding to snps ($IC_{50} = 7.69 \times 10^{-9}$ mol/L). The H_C domain of neither toxin contained all the snp binding sites of the toxin because each gave a maximum of 70% ($IC_{50} = 8.01 \times 10^{-9}$ mol/L) inhibition. The L chain had no inhibitory activity and hence could not be involved in cell surface interactions during binding and translocation, so no L chain peptides needed to be studied.

In earlier studies, Black and Dolly[19] showed that the toxin is internalized after binding to the cell surface receptor (acceptor) and that the process was temperature-dependent. The current studies confirmed aspects of the temperature dependency, but they also showed that the dependency varied with the contact

dx.doi.org/10.1021/bi201322c | Biochemistry 2012, 51, 316−328

Table 2. BoNT/B Peptides Involved in Interactions with Synaptosomes

Peptide Number	Residue Numbers	Amino acid sequence
H_N domain		
N6	512-530	**T D F N V** D V P V Y E K Q P **A I K K I**
N7	526-544	**A I K K I** F T D E N T I F Q **Y L Y S Q**
N12	596-614	**Q I V N D** F V I E A N K S N **T M D K I**
N15	638-656	**N F E N A** F E I A G A S I L **L E F I P**
N25	778-796	**C S V S Y** L M K K M I P L A **V E K L L**
H_C domain		
C3	876-894	**I D L S G** Y G A K V E V Y D **G V E L N**
C8	946-964	**I H N E Y** T I I N C M K N N **S G W K I**
C19	1100-1118	**M F N A G** N K N S Y I K L K **K D S P V**
C20	1114-1132	**K D S P V** G E I L T R S K Y **N Q N S K**
C21	1128-1146	**N Q N S K** Y I N Y R D L Y I **G E K F I**
C23	1156-1174	**I N D D I** V R K E D Y I Y L **D F F N L**
C24	1170-1188	**D F F N L** N Q E W R V Y T Y **K Y F K K**
C25	1184-1202	**K Y F K K** E E E K L F L A P **I S D S D**
C28	1226-1244	**K K D E E** S T D E I G L I G **I H R F Y**
C31	1268-1291	**K R K P Y** N L K L G C N W Q F I P K D E G W T E

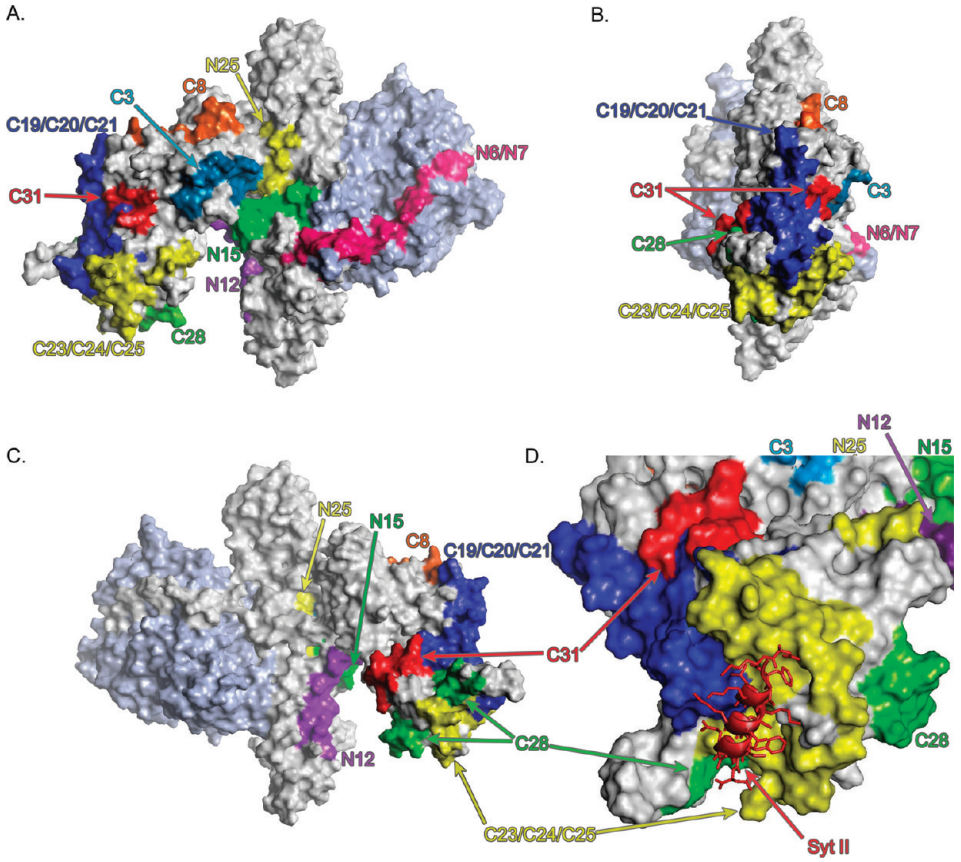

Figure 7. (A–C) Structural images of BoNT/B illustrating the accessible areas of all snp-binding regions mapped onto a surface representation of the BoNT/B three-dimensional structure. In the core BoNT/B structure, the H chain is colored white and the L chain light blue. The colored snp-binding regions correspond to those listed in Table 2 and are labeled with the identifying peptide numbers. Panel B is rotated ~90° around the *y*-axis, relative to panel A. Panel C is rotated ~90° relative to panel B. The three-dimensional coordinates are from PDB entry 1EPW.[62] (D) Illustration of the snp-binding regions mapped onto the surface of the BoNT/B–synaptotagmin II cocrystal structure. Portions of snp-binding regions C19–C21 (blue), C23–C25 (yellow), and C28 (green) form the synaptotagmin II binding pocket. In addition, C31 (red) is in the proximity of the ganglioside binding site as modeled by others.[24,25] All snp-binding regions within the C-terminal subdomain of H_C appear to be directly involved in receptor and/or ganglioside binding or are immediately proximal to those binding elements. The three-dimensional coordinates are from PDB entry 2NP0.[25]

regions of the toxin. These data also showed that BoNT/A and BoNT/B may bind to similar receptors as well as to serotype specific receptors. Li and Singh[64] proposed that BoNT/A, BoNT/B, and BoNT/E bind to synaptotagmin I. Our studies confirmed that BoNT/A and BoNT/B do compete for binding to snps, but the competition is not total. Each toxin can

Table 3. Comparison of the Regions on the BoNT/B H Chain That Are Recognized by Abs of Outbred Mice with the Snp-Binding Regions[a]

peptide	residues	mouse Abs	mouse brain snp binding
		H_N Domain	
N1	442−460	−	−
N2	456−474	−	−
N3	470−488	++	−
N4	484−502	+++	−
N5	498−516	−	−
N6	512−530	−	++
N7	526−544	−	+
N8	540−558	−	−
N9	554−572	−	−
N10	568−586	−	−
N11	582−600	−	−
N12	596−614	−	++
N13	610−628	−	−
N14	624−642	−	−
N15	638−656	++	+++
N16	652−670	−	−
N17	666−684	−	−
N18	680−698	−	−
N19	694−712	−	−
N20	708−726	−	−
N21	722−740	+	−
N22	736−754	+++	−
N23	750−768	−	−
N24	764−782	±	++
N25	778−796	+	−
N26	792−810	−	−
N27	806−824	−	−
N28	820−838	−	−
N29	834−852	−	−
		H_C Domain	
C1	848−866	++	−
C2	862−880	+	−
C3	876−894	−	+
C4	890−908	−	−
C5	904−922	−	−
C6	918−936	−	−
C7	932−950	++	−
C8	946−964	−	++
C9	960−978	−	−
C10	974−992	+++++	−
C11	988−1006	−	−
C12	1002−1020	−	−
C13	1016−1034	−	−
C14	1030−1048	++	−
C15	1044−1062	−	−
C16	1058−1076	+++	−
C17	1072−1090	+++	−
C18	1086−1104	−	−
C19	1100−1118	−	+
C20	1114−1132	−	++
C21	1128−1146	++	+++
C22	1142−1160	+++	−
C23	1156−1174	±	++
C24	1170−1188	−	++++
C25	1184−1202	−	+++
C26	1198−1216	++++	+
C27	1212−1230	−	−
C28	1226−1244	−	+
C29	1240−1258	+++	−
C30	1254−1272	−	−
C31	1268−1291	+++	+

[a]For the purpose of the table, the symbols for Ab binding are based on net counts per minute and denote the following: −, <1500 cpm; ±, 1500−3000 cpm; +, 3100−7000 cpm; ++, 7100−15000 cpm; +++, 15100−25000 cpm; ++++, 25100−35000 cpm; +++++, 35100−50000 cpm. Net counts per minute for mouse Abs were derived from the antiserum dilution that gave the highest level of binding.[32]

compete with the other to a maximum of ∼50%, and only part of that (29−32%) is performed by areas on the H_C domain, clearly indicating the remainder of the cross competition is through area(s) on the H_N domain.

To determine the snp-binding regions on the H chain of BoNT/B, we employed consecutive synthetic overlapping peptides that encompass the entire heavy chain and have a uniform size and fixed overlaps. The approach, introduced previously by this laboratory,[52−55] has been used for mapping a variety of immune and other recognition regions of continuous architecture (for a definition of continuous and discontinuous binding regions, see ref 56). We have employed this method for determining the locations of the continuous antibody and T cell recognition regions on BoNT/A and BoNT/B[32,51,57−60] and, particularly relevant to our study, for mapping the snp-binding regions on BoNT/A.[31] We prepared a panel of 29 H_N and 31 H_C 19-residue peptides (peptide C31 was 24 residues long) that overlapped consecutively by five residues and encompassed the entire H chain (residues 442−1291) (Table 1).

The inhibition studies at 37 °C revealed that binding regions of BoNT/B occur on the H_C and H_N domains of H. In addition to six binding regions found on the H_C domain within peptides C3, C8, C19−C21, C23−C25, C28, and C30, there are at least four binding regions on the H_N domain within peptides N6, N7, N12, N15, and N25 (see Figure 5 and Table 2 for a summary). The method does not allow definition of the exact boundaries of the sites but identifies the regions within which these sites reside. The highest inhibitory activity in H_N resided in peptide N15 followed by peptide N12, peptides N6 and N7, and peptide N25. On H_C, the highest inhibitory activity was exerted by the region(s) within peptides C23−C25 followed by the region(s) within peptides C20 and C21 and then peptide C8. Inhibition studies at 4 °C revealed that only peptide C24 retained very substantial inhibitory activity (31.2%) and peptides N15, C21, and C25 each retained an inhibitory activity that was just below 10%. It is tempting to conclude that the regions on the H_C domain participate in the initial binding to the cell surface and that the H_N domain provides contacts that are used during translocation. However, this is by no means certain as all these events obviously occur in vivo at 37 °C.

An equimolar mixture of the active peptides of H_N or H_C showed in each case a substantial additive effect (Figure 6), indicating that peptides are noncompeting and bind mostly to different binding sites or receptors. Surprisingly, however, a

dx.doi.org/10.1021/bi201322c | Biochemistry 2012, 51, 316−328

mixture of the active H_N and H_C peptides produced only a slightly higher level of inhibition than the mixture of only the H_C peptides. The reason for this is not easy to explain. It is likely caused by the concentration of each peptide in the 10-peptide mixture being lower than that in the H_N or H_C peptide. Also, the 10 active peptides find it difficult to neatly organize and bind correctly to the surface of the receptor(s) without encountering obstruction with each other or with nonbinding parts of other peptides.

The issue of how relatively small (19-residue) peptides can achieve a conformation that will be appropriate for binding needs to be addressed. At a given time, a peptide of this size will have a random-average conformation. A free peptide exists in solution in a conformational equilibrium among a number of conformational states, the time average of which is random. When one of these conformational states approaches a shape that is productive for binding, it will bind, and as it is thus removed, the equilibrium will shift in its favor. Therefore, in effect, the formation of a species with a favorable shape is induced by its ability to bind to a receptor. The molar excess of the peptide needed to achieve maximal inhibition was ~100-fold greater than the BoNT/B excess required for maximal inhibition. The aforementioned conformational equilibrium would explain the reason why a larger excess of peptide was needed for maximal inhibition.

To facilitate molecular analysis, the locations of the snp-binding peptides have been mapped onto the BoNT/B protein structure (see Figure 7A–C). The N6 and N7 region comprises approximately half of the H chain belt, specifically the portion of the belt that interacts with the L chain active site. Peptides N12, N15, and N25 are all contained within the helical bundle of the translocation domain and are proximal to the H_N–H_C interface. Of the 10 snp-binding peptides identified within the H_C domain, only two are in the N-terminal subdomain of the H_C, the remaining eight being located in the C-terminal subdomain. The mapped image is striking because a majority of the globular, C-terminal H_C subdomain is involved in snp binding. In addition, at least a portion of all snp-binding peptides can be accessed from one face of the elongated BoNT/B structure (see Figure 7A). The only peptides that are accessible from the opposite face are N12 and those in the C-terminal subdomain of H_C (i.e., C19–C21, C23–C25, C28, and C31) (see Figure 7C). The locations of the snp-binding regions on the BoNT/B structure did not correlate with hydrophobicity and/or hydrophilicity, surface electrostatic potential, or temperature factor (see the Supporting Information).

The presence of snp-binding regions on the H_C domain is expected on the basis of previous reports. Furthermore, mutation studies revealed that the carboxyl-terminal half of H_C of botulinum neurotoxins A and B has the binding elements of a single ganglioside-binding site.[61] The binding regions on BoNT/B for rat[24] or mouse[25] synaptotagmin II have been described and are present on the H_C domain of the toxin. The residues involved in ganglioside binding reside on the H_C domain as deduced from the structure of the complex of sialyllactose with BoNT/B.[62] The snp-binding regions are shown in relationship to the synaptotagmin II binding regions in Figure 7D. As expected, on the basis of the substantial snp binding characteristics mapped to the surface of the C-terminal half of the H_C, there is considerable overlap between the synaptotagmin II binding site and the snp-binding regions. In particular, the syt II and ganglioside binding pockets are comprised of at least portions of all the snp-binding regions within the H_{CC} domain (i.e., C28, C19–C21, C23–C25, and C31). The presence of snp-binding regions on the H_N domain, although unexpected from the prevailing view, is quite consistent with the in vitro and in vivo findings that the snp-binding regions on BoNT/A occur on the H_C and H_N domains of the H subunit.[31,63]

The possibility that some of the inhibitory activity of the H_N peptides might derive from their binding to H_C peptides needs to be considered. We employed the solvent accessibility calculation methods using the default radius of a water molecule (1.4 Å) and used standard or default values to determine whether a residue is solvent accessible. We have found that only N15 and N25 have a possibility of interacting with C3. On N15, residues N641 and E644 are H-bonded to K871. However, K871 is not on a mapped snp-binding H_C peptide, but it is near C3. When LH_N is analyzed, E644 is solvent-exposed when it is not in BoNT/B. Therefore, it is not likely that N15 will bind to C3. On N25, residue K785 H-bonds to S879 on C3 and residue K786 on N25 H-bonds to G880 on C3. However, when LH_N is analyzed, M784, K785, and P789 on N25 become solvent-exposed and V792 is no longer buried after removal of the H_C domain. It can be concluded that the activity of the H_N peptides is functionally authentic and important for BoNT/B binding and translocation.

It is relevant to compare the locations of the binding regions on BoNT/B for mouse snps with the binding regions for mouse blocking Abs. Table 3 compares the regions on the BoNT/B H chain that are recognized by blocking Abs of outbred mice[32] with the snp-binding regions found here, and Figure 8 shows this comparison graphically. Antibody-binding

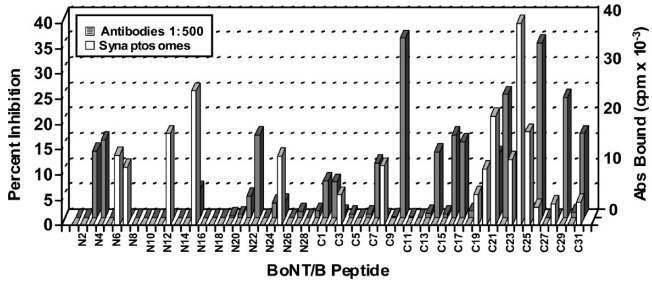

Figure 8. Comparative profiles of the BoNT/B H chain peptides that bind to mouse snps and those recognized by blocking (i.e., protecting) mouse anti-BoNT/B Abs. The antibody-binding regions have been described previously.[32]

regions within peptides N15, N24, C21, C23, C26, and C31 coincide completely with snp-binding regions within these peptides. In addition, Ab-binding regions on peptides N25, C7, C22, C26, and C29 overlap with snp-binding regions on the preceding or following overlapping peptides. Both the snp-binding and Ab-binding regions have been mapped onto the same BoNT/B structure to further demonstrate the considerable overlap between these binding characteristics (see Figure 9). Only three regions, comprised of peptides N6 and N7, N12, and C3, do not overlap within the primary sequence. However, upon analysis of the mapped binding regions, it is plausible that binding of Ab to regions that are remote in the primary sequence could inhibit snp binding even within the N6 and N7, N12, and C3 regions. This is due to the proximal location, in space, of these regions within the folded protein. For example, the surface accessible region of N15, which is bound by Abs, is close to all

dx.doi.org/10.1021/bi201322c | *Biochemistry* 2012, 51, 316–328

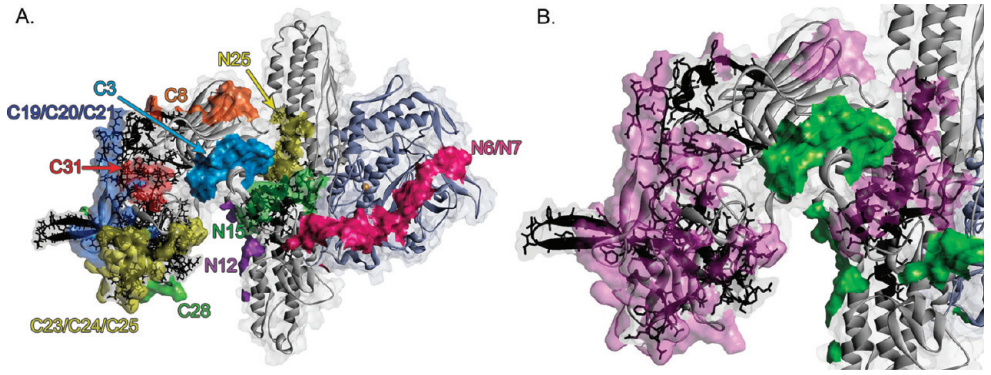

Figure 9. Structural representation of BoNT/B comparing the mouse snp-binding regions to the previously reported regions that are recognized and bound by blocking Abs of outbred mice.[32] In all views, the BoNT/B structure is illustrated with a transparent surface over a ribbon diagram with Ab-binding regions shown as a black ribbon (with side chains shown) and the remainder of the H chain ribbon colored white. Snp-binding regions are illustrated as colored surfaces and are transparent where there is overlap with Ab-binding regions. (A) Surface areas are colored differently to emphasize the snp-binding regions. Only the N6 and N7, N12, C3, and C8 regions do not directly overlap with Ab-binding regions. (B) Close-up with the snp-binding regions simplified by illustrating those that have overlap with Ab-binding regions as transparent pink and those that do not as solid green. The three-dimensional coordinates are from PDB entry 1EPW.[62]

three of the surface accessible regions that are not bound by Abs (i.e., N7, N12, and C3). It should be expected that Abs of sufficiently high affinity directed to these regions would block binding of these regions to the cell surface. This would explain how blocking Abs interfere with the activity of the toxin.

The snp-binding regions on BoNT/A have been identified,[31] and it should be of interest to compare the structural locations of these regions on BoNT/A and BoNT/B. The snp-binding regions of the two toxins are compared in Figure 10. It appears

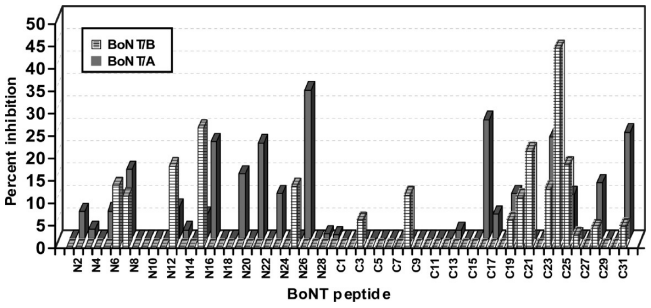

Figure 10. Comparison of the snp-binding regions located on the heavy chains of BoNT/B and BoNT/A. The levels of inhibition of binding of [^{125}I]BoNT/B to snps by synthetic peptides of the BoNT/B H chain or levels of inhibition of binding of [^{125}I]BoNT/A to snps by peptides of the BoNT/A H chain are shown as a bar diagram. The BoNT/A snp-binding regions have been identified previously.[31]

that BoNT/A has unique binding regions within BoNT/A peptides N19, N21, N23, and C16 while BoNT/B has distinctive binding regions within BoNT/B peptides C3, C8, C20, and C21. The remaining regions are comparable on the two toxins, and their primary structures are analyzed for homology in Table 4. The correlated regions within BoNT/A and BoNT/B peptides N6 and N7 or within peptides C23–C25 displayed low levels of homology and will probably not cross-react with the same snp-binding sites. The binding regions within peptides N26 of BoNT/A and N25 of BoNT/B had low levels of homology and would be expected to display little or no cross-reaction between them. The binding regions within N16 of BoNT/A and N15 of BoNT/B have complete identity of seven contiguous residues, and one residue removed, two more residues were identical. It is very likely that these sites could react with the same snp receptor, although perhaps with differing affinities. Levels of homology between the pairs of binding regions within C28 of BoNT/A and C28 of BoNT/B and between C31 peptides of the two toxins were fair, and it is likely that the correlated regions would have very low cross-reactivity and different affinities.

Analysis of the BoNT/A and BoNT/B tertiary structures with respect to the snp-binding regions (shown in Figure 11) reveals significant structural homology, even when the level of sequence homology is low (e.g., N26 of BoNT/A and N25 of BoNT/B). Even in instances where BoNT/A or BoNT/B has unique snp-binding sites, the unique sites are in regions that are proximal to other snp-binding sites. For example, while N19 of BoNT/A is on a different helix, the location is proximal to N16 of BoNT/A and N15 of BoNT/B. Likewise, N21 and N23 of BoNT/A are located within the same helical bundle region of H_N as the N12 binding site of BoNT/B. Within the C-terminal half of the H_C domain, analysis reveals that both the level of primary sequence and the level of tertiary structure homology of BoNT/A and BoNT/B are relatively low, likely a result of this subdomain containing the serotype specific protein and ganglioside receptor-binding regions. However, the analysis and supporting data clearly demonstrate this subdomain of both BoNTs is important for interaction with snps.

In conclusion, in the three-dimensional structure of BoNT/B, the snp-binding regions comprise a large area of the globule formed by the H_C domain as well as one face of the H_N domain and part of the belt on the same side of the molecule. The opposite (back) surface of H_N and the belt make a smaller contribution to binding. It would appear that the toxin binds to the cell surface through the head of the H_C globule and also employs regions primarily on one face of the H_N domain. The belt is also bound on one side and thus fixed on that side, while the other half of the loop around the light chain remains free, maintaining the flexibility to allow discharge of the light chain. The initial site of contact of the toxin with the cell surface cannot be determined in these experiments because they do not allow insight into the sequence of events that take place during this process, but it is likely that the toxin binds to snps through

dx.doi.org/10.1021/bi201322c | *Biochemistry* 2012, 51, 316–328

Table 4. Homologies of Snp-Binding Regions on BoNT/A and BoNT/B[a]

BoNT/A N6-N7(519–551)	NLSSDIIG QLELMPNIERFPNGKKYELDKYTMF
BoNT/B N6-N7(512–544)	TDFNVDV PVYEKQPAIKKIFTDENTIFQYLYSQ
BoNT/A N16(659–677)	SGAVILLEFIPEIAIPVLG
BoNT/B N15(638–656)	NFENAFEIAGASILLEFIP
BoNT/A N26(799–817)	SMIPYGVKRLEDFDASLKD
BoNT/BN25(778–796)	CSVSYLMKKMIPLAVEKLL
BoNT/A C23-C24(1163-1195)	KKYASGNKDNIVRNND RVYINVVVKN KEYRLAT
BoNT/B C23-C24(1156-1188)	INDDIVRKEDYIYLDFFNLNQEWRVYTY KYFKK
BoNT/A C25 (1196-1209)	NASQAGVEKI LSAL
BoNT/B C25 (1189-1202)	EE EKLFL APISDSD
BoNT/A C281233-1251	NKCKMNLQDNNGNDIGFIG
BoNT/B C28 1226-1244	KKD EEST DEIGLIGIHRFY
BoNT/A C31 1275-1296	SRT LGCSWEFIPVDDGWGERPL
BoNT/B C31 1268-1291	KRKPYNLKLGCNWQFIPKDEGWTE

[a]Identical residues are shown in bold. Residues with functionally equivalent side chains are shown in bold italics. Gaps are introduced to maximize homologies. The table shows only the regions that occur in equivalent structural locations. The regions that are unique to each BoNT serotype are not displayed. The snp-binding regions of BoNT/A have been described previously.[31]

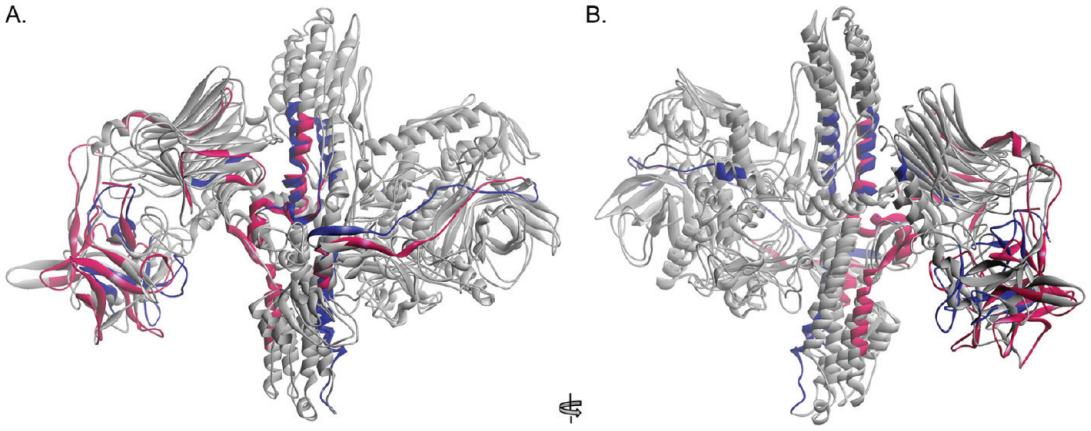

Figure 11. Overlay of the BoNT/A and BoNT/B structures to compare the snp-binding regions of BoNT/B (this study) to the previously reported snp-binding regions of BoNT/A.[31] Both BoNT/A and BoNT/B are illustrated as white ribbons. Snp-binding regions of BoNT/A and BoNT/B are colored blue and magenta, respectively. There is clear overlap in the snp-binding regions mapped to the two different BoNT serotypes. Panel B is rotated ~180° around the *y*-axis, relative to panel A. The three-dimensional coordinates are from PDB entry 3BTA[65] for BoNT/A and PDB entry 1EPW[62] for BoNT/B.

the head of H_C and employs additional regions on one face of the H_N domain during translocation.

■ ASSOCIATED CONTENT

Supporting Information

Locations in the three-dimensional structure of the synaptosome-binding regions on BoNT/B in relation to hydophilicity and hydrophobicity, charge distribution, and temperature factor (motion) of the surface. This material is available free of charge via the Internet at http://pubs.acs.org.

■ AUTHOR INFORMATION

Corresponding Author

*One Baylor Plaza, Houston, TX 77030. Telephone: (713) 798-6050. Fax: (713) 798-6437. E-mail: matassi@bcm.tmc.edu.

Funding

This work was supported by an unrestricted research grant from Allergan, Inc., and by Welch Foundation Grant Q007 to M.Z.A., who is the Robert A. Welch Chair of Chemistry.

■ ACKNOWLEDGMENTS

We are grateful to Dr. Leonard A. Smith (U.S. Army Medical Research and Materiel Command) for recombinant BoNT/B H_C and L chain. The excellent technical assistance of Ms. Masooma R. Naqvi is also gratefully acknowledged.

■ ABBREVIATIONS

Ab, antibody; BSA, bovine serum albumin; BoNT, botulinum neurotoxin; BoNT/A, botulinum neurotoxin A; BoNT/B, botulinum neurotoxin B; C1−C31, synthetic H_C domain peptides of BoNT/B; H, heavy chain of BoNT/B; H_N, N-terminal domain (residues 442−852) of the H chain; H_C, C-terminal domain (residues 848−1291) of the H chain; N1−N29, synthetic H_N domain peptides of BoNT/B; PBS, 0.01 M sodium phosphate and 0.15 M NaCl (pH 7.2); snps, synaptosomes; syt II, synaptotagmin II; PDB, Protein Data Bank.

■ REFERENCES

(1) Fu, F. N., Lomneth, R. B., Cai, S., and Singh, B. R. (1998) Role of zinc in the structure and toxic activity of botulinum neurotoxin. *Biochemistry* 37, 5267−5278.

(2) Aoki, K. R., Smith, L. A., and Atassi, M. Z. (2010) Mode of action of botulinum neurotoxins. Current vaccination strategies and molecular immune recognition of the toxin. *Crit. Rev. Immunol. 30*, 167−187.
(3) Pellizzari, R., Rossetto, O., Schiavo, G., and Montecucco, C. (1999) Tetanus and botulinum neurotoxins: Mechanism of action and therapeutic uses. *Philos. Trans. R. Soc. London, Ser. B 354*, 259−268.
(4) Agui, T., Syuto, B., Oguma, K., Iida, H., and Kubo, S. (1983) Binding of *Clostridium botulinum* type C neurotoxin to rat brain synaptosomes. *J. Biochem. 94*, 521−527.
(5) Kitamura, M. (1976) Binding of botulinum neurotoxin to the synaptosome fraction of rat brain. *Naunyn-Schmiedeberg's Arch. Pharmacol. 295*, 171−175.
(6) Kozaki, S. (1979) Interaction of botulinum type A, B and E derivative toxins with synaptosomes of rat brain. *Naunyn-Schmiedeberg's Arch. Pharmacol. 308*, 67−70.
(7) Kozaki, S., and Sakaguchi, G. (1982) Binding to mouse brain synaptosomes of *Clostridium botulinum* type E derivative toxin before and after tryptic activation. *Toxicon 20*, 841−846.
(8) Kohda, T., Kamata, Y., and Kozaki, S. (2000) Endocytosis of *Clostridium botulinum* type B neurotoxin into rat brain synaptosomes. *J. Vet. Med. Sci. 62*, 1133−1138.
(9) Li, L., and Singh, B. R. (1999) In vitro translocation of type A *Clostridium botulinum* neurotoxin heavy chain and analysis of its binding to rat synaptosomes. *J. Protein Chem. 18*, 89−95.
(10) Nishiki, T., Kamata, Y., Nemoto, Y., Omori, A., Ito, T., Takahashi, M., and Kozaki, S. (1994) Identification of protein receptor for *Clostridium botulinum* type B neurotoxin in rat brain synaptosomes. *J. Biol. Chem. 269*, 10498−10503.
(11) Nishiki, T., Tokuyama, Y., Kamata, Y., Nemoto, Y., Yoshida, A., Sekiguchi, M., Takahashi, M., and Kozaki, S. (1996) Binding of botulinum type B neurotoxin to Chinese hamster ovary cells transfected with rat synaptotagmin II cDNA. *Neurosci. Lett. 208*, 105−108.
(12) Nishiki, T., Tokuyama, Y., Kamata, Y., Nemoto, Y., Yoshida, A., Sato, K., Sekiguchi, M., Takahashi, M., and Kozaki, S. (1996) The high-affinity binding of *Clostridium botulinum* type B neurotoxin to synaptotagmin II associated with gangliosides GT1b/GD1a. *FEBS Lett. 378*, 253−257.
(13) Najib, A., Pelliccioni, P., Gil, C., and Aguilera, J. (1999) *Clostridium* neurotoxins influence serotonin uptake and release differently in rat brain synaptosomes. *J. Neurochem. 72*, 1991−1998.
(14) Schengrund, C. L., DasGupta, B. R., Hughes, C. A., and Ringler, N. J. (1996) Ganglioside-induced adherence of botulinum and tetanus neurotoxins to adducing. *J. Neurochem. 66*, 2556−2561.
(15) Arribas, M., Blasi, J., Egea, G., Farinas, I., Solsona, C., and Marsal, L. (1993) High resolution labeling of cholinergic nerve terminals using a specific fully active biotinylated botulinum neurotoxin type A. *J. Neurosci. Res. 36*, 635−645.
(16) Morel, N., Israel, M., Manaranche, R., and Mastour-Franchon, P. (1977) Isolation of pure cholinergic nerve endings from *Torpedo* electric organ. Evaluation of their metabolic properties. *J. Cell Biol. 75*, 43−55.
(17) Hirokawa, N., and Kitamura, M. (1979) Binding of *Clostridium botulinum* neurotoxin to the presynaptic membrane in the central nervous system. *J. Cell Biol. 81*, 43−49.
(18) Dolly, J. O., Williams, R. S., Black, J. D., Tse, C. K., Hambleton, P., and Melling, J. (1982) Localization of sites for ^{125}I-labeled botulinum neurotoxin at murine neuromuscular junction and its binding to rat brain synaptosomes. *Toxicon 20*, 141−148.
(19) Black, J. D., and Dolly, J. O. (1986) Interaction of ^{125}I-labeled botulinum neurotoxins with nerve terminals. II. Autoradiographic evidence for its uptake into motor nerves by acceptor-mediated endocytosis. *J. Cell Biol. 103*, 535−544.
(20) Kozaki, S., Kamata, Y., Watarai, S., Nishiki, T., and Mochida, S. (1998) Ganglioside GT1b as a complementary receptor component for *Clostridium botulinum* neurotoxins. *Microb. Pathog. 25*, 91−99.
(21) Bakry, N. M., Kamata, Y., and Simpson, L. L. (1997) Expression of botulinum toxin binding sites in *Xenopus* oocytes. *Infect. Immun. 65*, 2225−2232.
(22) Dong, M., Richards, D. A., Goodnough, M. C., Tepp, W. H., Johnson, E. A., and Chapman, E. R. (2003) Synaptotagmins I and II mediate entry of botulinum neurotoxin B into cells. *J. Cell Biol. 162*, 1293−1303.
(23) Ihara, H., Kohda, T., Morimoto, K., Tsukamoto, K., Karazawa, T., Nakamura, S., Mukamoto, M., and Kozaki, S. (2003) Sequence of the gene for *Clostridium botulinum* type B neurotoxin associated with infant botulism, expression of the C-terminal half of heavy chain and its binding activity. *Biochim. Biophys. Acta 1625*, 19−26.
(24) Jin, R., Rummel, A., Binz, T., and Brunger, A. T. (2006) Botulinum neurotoxin B recognizes its protein receptor with high affinity and specificity. *Nature 444*, 1092−1095.
(25) Chai, Q., Arndt, J. W., Dong, M., Tepp, W. H., Johnson, E. A., Chapman, E. R., and Stevens, R. C. (2006) Structural basis of cell surface receptor recognition by botulinum neurotoxin B. *Nature 444*, 1096−1100.
(26) DasGupta, B. R., and Sugiyama, H. A. (1972) A common subunit structure in *Clostridium botulinum* type A, B and E toxins. *Biochem. Biophys. Res. Commun. 48*, 108−112.
(27) Bandyopadhyay, S., Clark, A. W., Das Gupta, B., and Sathyamoorthy, V. (1987) Role of the heavy and light chains of botulinum neurotoxin in neuromuscular paralysis. *J. Biol. Chem. 262*, 2660−2663.
(28) Kozaki, S., Miki, A., Kamata, Y., Ogasawara, J., and Sakaguchi, G. (1989) Immunological characterization of papain-induced fragments of *Clostridium botulinum* type A neurotoxin and interaction of the fragments with brain synaptosomes. *Infect. Immun. 57*, 2634−2639.
(29) Shone, C. C., Hambleton, P., and Melling, J. (1985) Inactivation of *Clostridium botulinum* type A neurotoxin by trypsin and purification of two tryptic fragments. Proteolytic action near the COOH-terminus of the heavy subunit destroys toxin-binding activity. *Eur. J. Biochem. 15*, 75−82.
(30) Gimenez, J. A., and DasGupta, B. R. (1993) Botulinum type A neurotoxin digested with pepsin yields 132, 97, 72, 45, 42, and 18 kD fragments. *J. Protein Chem. 12*, 351−363.
(31) Maruta, T., Dolimbek, B. Z., Aoki, K. R., Steward, L. E., and Atassi, M. Z. (2004) Mapping of the synaptosome-binding regions on the heavy chain of botulinum neurotoxin A by synthetic overlapping peptides encompassing the entire chain. *Protein J. 23*, 539−552.
(32) Dolimbek, B. Z., Steward, L. E., Aoki, K. R., and Atassi, M. Z. (2008) Immune recognition of botulinum neurotoxin B: Antibody-binding regions on the heavy chain of the toxin. *Mol. Immunol. 45*, 910−924.
(33) Whittaker, V. P. (1959) The isolation and characterization of acetylcholine-containing particles from brain. *Biochem. J. 72*, 694−706.
(34) Bradford, M. M. (1976) A rapid and sensitive method for the quantitation of microgram quantities of protein utilizing the principle of protein-dye binding. *Anal. Biochem. 72*, 248−254.
(35) Hunter, W. M., and Greenwood, F. C. (1962) Preparation of iodine-131 labeled human growth hormone of high specific activity. *Nature 194*, 495−496.
(36) Atassi, M. Z., and Oshima, M. (1999) Structure, activity, and immune (T and B cell) recognition of botulinum neurotoxins. *Crit. Rev. Immunol. 19*, 219−260.
(37) Jankovic, J. (2004) Botulinum toxin in clinical practice. *J. Neurol., Neurosurg. Psychiatry 75*, 951−957.
(38) Jankovic, J. (2006) Botulinum toxin therapy for cervical dystonia. *Neurotox. Res. 9*, 145−148.
(39) Silberstein, S. D. (2001) Review of botulinum toxin type A and its clinical applications in migrane headache. *Expert Opin. Pharmacother. 2*, 1649−1654.
(40) Borodic, G. E., Acquardo, M., and Johnson, E. A. (2001) Botulinum toxin therapy for pain and inflammatory disorders: Mechanisms and therapeutic effects. *Expert Opin. Invest. Drugs 10*, 1531−1544.

(41) Becker-Wegerich, P. M., Rauch, L., and Ruzicka, T. (2002) Botulinum toxin A: Successful decollete rejuvenation. *Dermatol. Surg. 28*, 168−171.
(42) Binder, W. J., Brin, M. F., Blitzer, A., and Pogoda, J. M. (2002) Botulinum toxin type A (BOTOX) for treatment of migraine. *Dis. Monitor. 48*, 323−335.
(43) Turton, K., Chaddock, J. A., and Acharya, K. R. (2002) Botulinum and tetanus neurotoxins: Structure, function and therapeutic utility. *Trends Biochem. Sci. 27*, 552−558.
(44) Gui, D., Rossi, S., Runfola, M., and Magalini, S. C. (2003) Review article: Botulinum toxin in the therapy of gastrointestinal motility disorders. *Aliment. Pharmacol. Ther. 18*, 1−16.
(45) Pickett, A. (2010) Re-engineering clostridial neurotoxins for the treatment of chronic pain: Current status and future prospects. *BioDrugs 24*, 173−182.
(46) Atassi, M. Z. (2004) Basic immunological aspects of botulinum toxin therapy. *Movement Disorders 19*, S68−S84.
(47) Jankovic, J. (2002) Botulinum toxin: Clinical implications of antigenicity immunoresistance. In *Scientific, Therapeutic Aspects of Botulinum Toxin* (Brin, M. F., Hallett, M., and Jankovic, J., Eds.) pp 409−415, Lippincott, Williams and Wilkins, Philadelphia.
(48) Jankovic, J., Hunter, C., Dolimbek, B. Z., Dolimbek, G. S., Adler, C. H., Brashear, A., Comella, C. L., Gordon, M., Riley, D. E., Sethi, K., Singer, C., Stacy, M., Tarsy, D., and Atassi, M. Z. (2006) Clinico-immunologic aspects of botulinum toxin type B treatment of cervical dystonia. *Neurology 67*, 2233−2235.
(49) Atassi, M. Z., Ruan, K. H., Jinnai, K., Oshima, M., and Ashizawa, T. (1992) Epitope-specific suppression of antibody response in experimental autoimmune myasthenia gravis by a monomethoxypolyethylene glycol conjugate of a myasthenogenic synthetic peptide. *Proc. Natl. Acad. Sci. U.S.A. 89*, 5852−5856.
(50) Dolimbek, B. Z., Aoki, K. R., and Atassi, M. Z. (2011) Reduction of antibody response against botulinum neurotoxin A by synthetic monomethoxypolyethylene glycol-peptide conjugates. *Immunol. Lett. 137*, 46−52.
(51) Atassi, M. Z., Dolimbek, B. Z., Jankovic, J., Steward, L. E., and Aoki, K. R. (2008) Molecular recognition of botulinum neurotoxin B heavy chain by human antibodies from cervical dystonia patients that develop immunoresistance to toxin treatment. *Mol. Immunol. 45*, 3878−3888.
(52) Kazim, A. L., and Atassi, M. Z. (1980) A novel and comprehensive synthetic approach for the elucidation of protein antigenic structures. Determination of the full antigenic profile of the α-chain of human haemoglobin. *Biochem. J. 191*, 261−264.
(53) Kazim, A. L., and Atassi, M. Z. (1982) Structurally inherent antigenic sites. Localization of the antigenic sites of the α-chain of human haemoglobin in three host species by a comprehensive synthetic approach. *Biochem. J. 203*, 201−208.
(54) Bixler, G. S., Yoshida, T., and Atassi, M. Z. (1984) T cell recognition of lysozyme. IV. Localization and genetic control of the continuous T cell recognition sites by synthetic overlapping peptides representing the entire protein chain. *J. Immunogenet. 11*, 327−337.
(55) Bixler, G. S., and Atassi, M. Z. (1984) T cell recognition of myoglobin. Localization of the sites stimulating T cell proliferative responses by synthetic overlapping peptides encompassing the entire molecule. *J. Immunogenet. 11*, 339−353.
(56) Atassi, M. Z., and Smith, J. A. (1978) A proposal for the nomenclature of antigenic sites in peptides and proteins. *Immunochemistry 15*, 609−610.
(57) Atassi, M. Z., Dolimbek, B. Z., Hayakari, M., Middlebrook, J. L., Whitney, B., and Oshima, M. (1996) Mapping of the antibody-binding regions on botulinum neurotoxin H-chain domain 855−1296 with antitoxin antibodies from three host species. *J. Protein Chem. 15*, 691−700.
(58) Oshima, M., Hayakari, M., Middlebrook, J. L., and Atassi, M. Z. (1997) Immune recognition of botulinum neurotoxin type A: Regions recognized by T cells and antibodies against the protective H(C) fragment (residues 855−1296) of the toxin. *Mol. Immunol. 34*, 1031−1040.
(59) Atassi, M. Z., and Dolimbek, B. Z. (2004) Mapping of the Antibody-Binding Regions on the HN-Domain (Residues 449−859) of Botulinum Neurotoxin A with Antitoxin Antibodies from Four Host Species. Full Profile of the Continuous Antigenic Regions of the H-Chain of Botulinum Neurotoxin A. *Protein J. 23*, 39−52.
(60) Dolimbek, G. S., Dolimbek, B. Z., Aoki, K. R., and Atassi, M. Z. (2005) Mapping of the antibody and T cell recognition profiles of the HN domain (residues 449−859) of the heavy chain of botulinum neurotoxin A in two high-responder mouse strains. *Immun. Invest. 34*, 119−142.
(61) Rummel, A., Mahrhold, S., Bigalke, H., and Binz, T. (2004) The HCC-domain of botulinum neurotoxins A and B exhibits a singular ganglioside binding site displaying serotype specific carbohydrate interaction. *Mol. Microbiol. 51*, 631−643.
(62) Swaminathan, S., and Eswaramoorthy, S. (2000) Structural analysis of the catalytic and binding sites of *Clostridium botulinum* neurotoxin B. *Nat. Struct. Biol. 7*, 693−699.
(63) Atassi, M. Z., Dolimbek, B. Z., Steward, L. E., and Aoki, K. R. (2010) Inhibition of botulinum neurotoxin A toxic action in vivo by synthetic synaptosome- and blocking antibody-binding regions. *Protein J. 29*, 320−327.
(64) Li, L., and Singh, B. R. (1998) Isolation of synaptotagmin as a receptor for types A and E botulinum neurotoxin and analysis of their comparative binding using a new microtiter plate assay. *J. Nat. Toxins 7* (3), 215−226.
(65) Lacy, D. B., Tepp, W., Cohen, A. C., DasGupta, B. R., and Stevens, R. C. (1998) Crystal structure of botulinum neurotoxin type A and implications for toxicity. *Nat. Struct. Biol. 5*, 898−902.